

Chemical Deposition of Nickel Platinum Alloy on the Surface of TiO₂ Nanotubes as a Catalyst for Methanol Oxidation

Mohamed A. Ghanem^{1,2,*}, Abdullah M. Al-Mayouf^{1,2}, Maged N. Shaddad¹, Mansour S. Alhoshan^{2,3}
Mater N. Al-Shalawi¹

¹ Chemistry Department, College of Science, King Saud University, Riyadh 11451, KSA.

² Sustainable Energy Technologies (SET), King Saud University, Riyadh, KSA.

³ Chemical Engineering Department, Engineering College, King Saud University, KSA.

* E-mail: mghanem@ksu.edu.sa

Received: 22 December 2014 / Accepted: 10 February 2015 / Published: 24 February 2015

This work demonstrates the chemical deposited of nickel platinum alloy NiPt/TONs on the surface of titanium oxides nanotubes (TONs) support pre-fabricated by anodic oxidation of Ti foil in HF solution followed by annealing in air and in N₂ atmosphere. The structural, surface morphology and composition of NiPt/TONs catalysts were characterized using X-ray diffraction (XRD), scanning electron microscopy (SEM), energy dispersive X-ray spectroscopy (EDS) and the inductive coupled plasma optical emission spectroscopy (ICP-OES). The electrochemical behavior and methanol catalytic performance and stability of the NiPt/TONs catalysts were investigated by cyclic voltammetry and compared with similar catalysts in acidic and alkaline solutions. The results indicate that the NiPt/TONs shows higher catalytic activity for methanol electro-oxidation in both acidic and alkaline solution than that reported in the literature. This implies that TONs have promising potential to be used as a support for catalysis applications.

Keywords: Chemical deposition, TiO₂ nanotubes array, NiPt catalyst, cyclic voltammetry, Methanol electrooxidation.

1. INTRODUCTION

Titanium oxide nanotubes TONs offers interesting semiconducting properties, chemical inertness and stability, cost effectiveness and corrosion resistance [1,2,3,4], and is used in many fields, such as photocatalysis [5,6,7], solar cells, electronic devices, and environmental cleaning and protection [8,9]. For application as electrochemical electrodes [10,11], the TONs have advantages of they are readily attached to the titanium substrate and form oriented, aligned and perpendicular arrays which provides much improved electron transfer and mass transport pathways [12].TONs arrays

prepared by anodization usually exhibit relatively low electrical conductivity [13] which limits their applications in electro-catalysis and as catalyst supports. Therefore, several methods are often adopted to improve the electrical conductivity and reactivity of TONs structures by generating oxygen vacancies and metal or non-metal doping to satisfy the requirements for effective electrode materials. Annealing in different gas atmospheres is considered to be one feasible approach to narrow the band gap and enhance the electrical conductivity of TONs [14,15]. Noble metals, such as Au [16], Pt [17], Ag [18], and Pd [19], were incorporated as a co-catalyst onto the surface of TONs to enhance the electrons transfer, photocatalytic activity and carriers charge separation. Ag and Au nanoparticles were found to significantly enhance the photocatalytic activity of TiO₂ nanotubular structures [20].

Transition metal of Ni [21,22] and Ni/Cu nanoparticles modified TiO₂ [23] have also attracted considerable attention due to their potential use in catalysts and photoelectrochemical materials [24]. The synthesis of Ni nanoparticle-loaded TiO₂ grains has been reported [25,26,27]. One method for loading Ni nanoparticles on TiO₂ nanotube (Ni/TiO₂NTs) arrays is via pulsed electrodeposition method and under illumination, the produce Ni/TiO₂NTs exhibits remarkably enhanced the catalytic activity and stability for methanol oxidation in alkaline media [28,29,30,31].

A platinum (Pt) nanoparticle supported titania (TiO₂) nanotube arrays (Pt/TiO₂-NTs) has been successfully fabricated on Ti mesh via a thermal reduction of pre-spraying of H₂PtCl₆. 6H₂O isopropanol solution onto vertically oriented TiO₂ nanotube arrays. Investigations showed that the Pt/TiO₂ NTs electrode has superior electrocatalytic activity, good stability, and low ohmic resistance (3.41 Ω cm²) [32]. Au nanoparticles also dispersed over a self-organized nanotubular TiO₂ matrix shows highly efficient catalyst system for the electrochemical oxygen reduction reaction in aqueous solutions. The nanotubular support significantly enhances the activity of the TiO₂/Au system in comparison with the flat TiO₂ layers [33]. In other study, Cu(OH)₂/TiO₂ photocatalyst was prepared by loading different amounts of Cu(OH)₂ nanoparticles on TiO₂ nanotube arrays (TiO₂-NTs) using a chemical deposition method. The prepared catalyst was used to generate hydrogen under simulated solar light irradiation, and the results demonstrated that the hydrogen yield of Cu(OH)₂/TiO₂-NTs was over twenty times that of the pure TiO₂-NT indicating that Cu(OH)₂/TiO₂-NTs photocatalyst showed excellent stability and reusability [34].

Electroless deposition of nickel is usually classified according to the nature of the reducing agent. Nickel–phosphorous deposits (based on reduction by the hypophosphite ion) are the most studied and used but the properties of nickel–boron deposits are of very great interest for several industrial applications [35]. Most of the studies focused on electroless deposition of nickel and particularly on nickel–boron describing the optimization of plating parameters, the coating properties or the effect of heat treatment [36]. Recently Ni-B coatings were used as electrocatalyst for electrocatalytic oxidation of alcohols and it was found that the nanostructured Ni-B alloy had higher electrocatalytic activity for the oxidation of methanol than the electroless deposited amorphous Ni-B alloy electrode [37].

Recently we reported the deposition of platinum [38], gold and platinum gold [39] nanoparticles supported on TiO₂ nanotubes which show enhanced higher catalytic activity for the oxygen reduction, hydrogen evolution and methanol oxidation reactions. This work demonstrates the electroless deposition of nickel platinum NiPt catalysts supported on TONs arrays using chemical bath

deposition. The produced NiPt/TONs catalysts were annealed in air and N₂ atmospheres to improve the electrical conductivity and performance of catalysts. The effect of deposition time and the annealing of TONs on different gas on the dispersion, particle size and electrocatalytic properties of the NiPt/TONs catalysts were investigated.

2. EXPERIMENTAL

2.1 Chemical and materials

Ti foil (purity > 99.5% thickness 0.25 mm), dihydrogen hexachloroplatinate (IV) hydrate (H₂PtCl₆.6H₂O > 99.99%), Nickel sulphate (NiSO₄.6H₂O > 99%) and PdCl₂ (purity > 99.99%) were purchase from Alfa Aesar. HF (purity 39-43%) from QualiKems, NaBH₄ (purity > 98.0%, WINLAB), NH₂NH₂ (> 99.0%) and C₂H₄(NH₂)₂ (> 99.0%) were obtained from PS. H₂SO₄ (> 98.0%, BDH, AR), CH₃OH (purity > 99.5%, AVONCHEA, AR), NaOH (Fluka), SnCl₂.2H₂O (Sigma Aldrich, ACS reagent) and HNO₃ (purity >99.0%, BDH, AR). All reagents were of analytical grade and used without further purification. All aqueous solutions were prepared using Milli-Q (Millipore, Inc.) high quality deionized (DI) water (resistance 18.2 MΩ cm).

2.2 Synthesis of TONs substrate and catalysts

TONs were synthesized by anodization following the procedure reported in our previous work [38]. In summary pure titanium foils (2×3 cm²) (0.25 mm thick, purity 99.5%, Alfa Aesar) was ultrasonically washed with acetone, isopropanol and distilled water. Then the titanium substrates were anodized in 0.5 wt% hydrofluoric (HF) acid at 20 V for 20 min in two electrode cell with platinum foil (2 x 2 cm²) as a cathode.

Table 1. Composition and experimental condition of the NiPt electroless plating bath.

Composition	Concentration/ M
H ₂ PtCl ₆ .6H ₂ O	0.026
NiSO ₄ .6H ₂ O	0.026
C ₂ H ₄ (NH ₂) ₂	0.059
NaBH ₄	0.106
pH	13.0 ± 0.2
Temperature	60.0 ± 2.0 °C

After the TONs arrays were annealed at 450 °C for 3.0 h in ambient air and in pure N₂-gas stream. Subsequently, the NiPt/TONs catalyst was prepared by a three step procedure; (i) the TONs were sensitization in a solution prepared by mixing 0.3 wt. % SnCl₂ + 3.0 wt. % HCl, for 30 min followed by washing with distilled water and dried at room temperature, (ii) the sensitized TONs were activated in a solution prepared by mixing 0.1 wt.% PdCl₂ + 2.0 wt.% HCl for 30 min followed by washing by distilled water and finally the TONs substrates were immersed in plating bath for nickel platinum alloy deposition. The composition of NiPt alloy chemical deposition bath is shown in table 1. After the electroless deposition was complete, the catalysts was washed with distilled water and dried at room temperature.

Characterizations TONs substrates and NiPt/TONs catalysts were characterized by XRD (Ultima IVX-ray diffractometer, Rigaku) with Cu-K_α radiation source ($\lambda = 1.54 \text{ \AA}$, 40 kV, 40 mA) and the diffraction pattern was measured at the scan rate of 0.03 deg s⁻¹. The surface morphology of the catalysts was examined by high resolution scanning electron microscope (SEM, JSM-6380LA) with integrated energy dispersive X-ray spectroscopy (EDS) (Vantage 4105, NORAN). The composition analysis of catalysts was determined by using an inductively coupled plasma optical emission spectroscopy (ICP-OES) system (Thermo Scientific; UK, Model ICAP 6000). For this purpose, the catalysts were dissolved in HNO₃ acid (E-Merck) using high-pressure microwave digestion system (MAR SX; CEM). The electrochemical characterizations were performed in three-electrode single-compartment Pyrex glass cell using a computerized potentiostat/galvanostat (Autolab, PGSTAT30). The reference and the auxiliary electrodes were SCE and 1.0 cm² platinum-foil, respectively.

3. RESULTES AND DISCUSSION

3.1 Characterization of NiPt-TONs catalysts

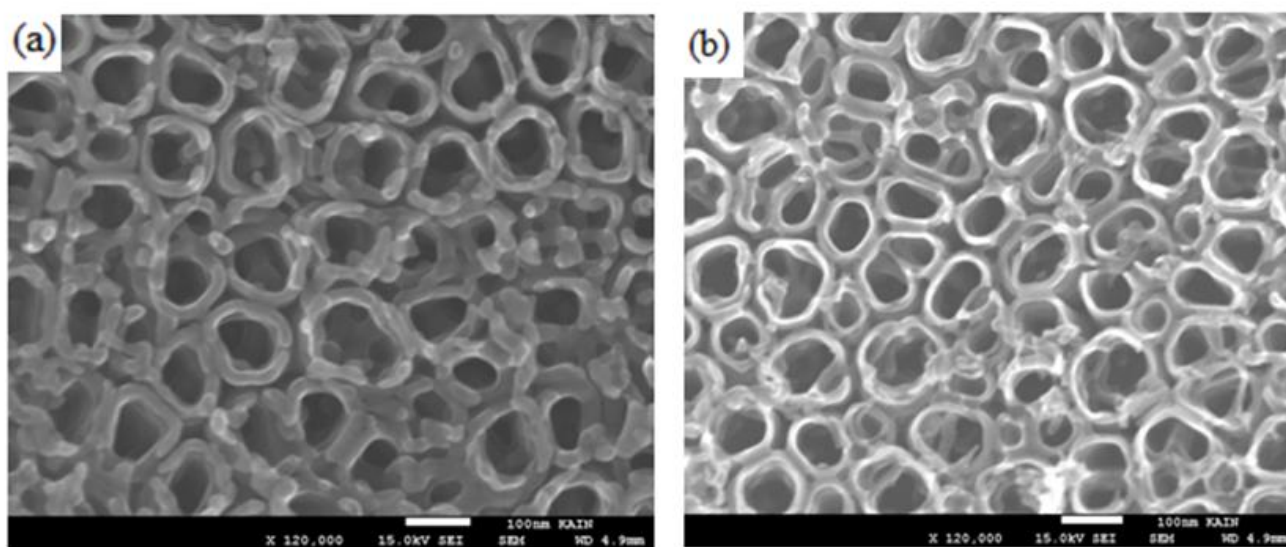


Figure 1. SEM images of (a) TONs annealing in air and (b) TONs annealing in N₂ at at 450 °C for 3.0 hours.

Figure 1 shows the SEM images of the TONs arrays annealed in ambient air (TONs-air) and in N_2 (TONs- N_2) atmospheres at 450 °C for 3.0 hours. From the visual observation the grey color of the as-prepared TONs was changed to grey yellow and dark blue in case of TONs- N_2 and TONs-air respectively. This indicates on some structure change in TONs due to annealing in air and nitrogen atmosphere. From the SEM images, the measured wall thickness for the TONs-air is about 30 nm whereas the wall thickness for the TONs- N_2 is ~ 9 nm indicating on structure expansion and compression respectively. As expected, the increase of wall thickness was accompanied with a decrease in the length of TONs which is consistent with the reported literatures [40]. In addition the TONs packing density (number of TONs/ unit area) is increased in case of TONs- N_2 leading to an increase in the surface area of TONs- N_2 .

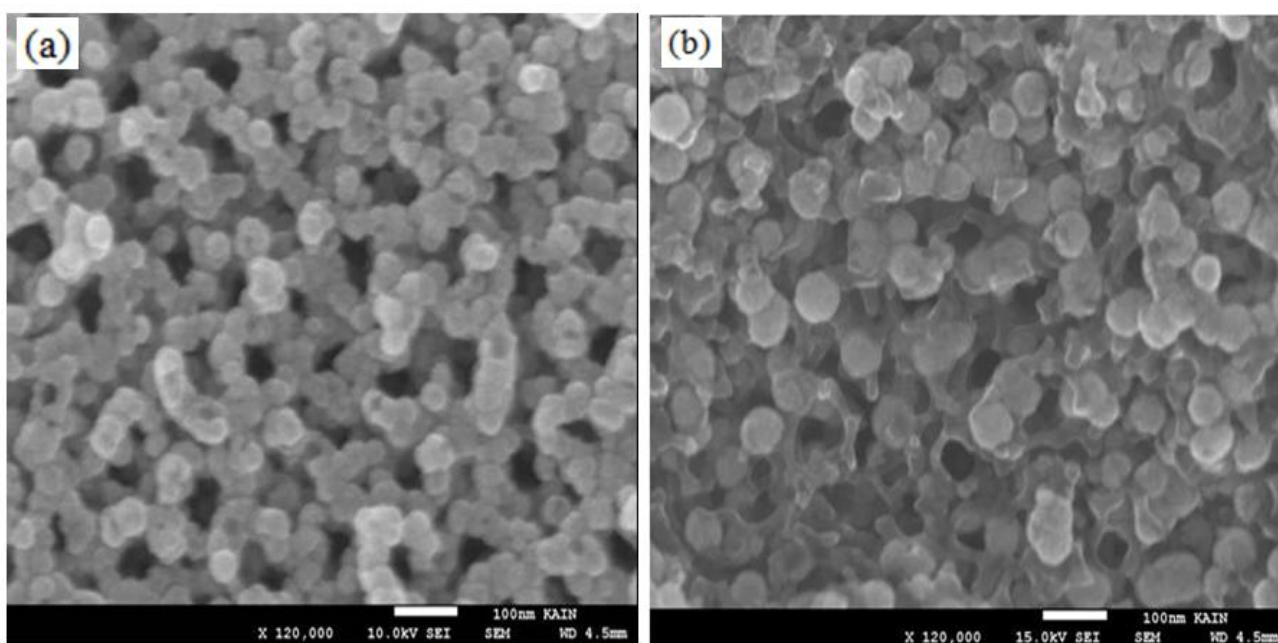


Figure 2. SEM images for (a) NiPt/TONs-air, (b) NiPt/TONs- N_2 , at deposition time of 30 min.

Figure 2 shows the SEM images for NiPt/TONs-air and NiPt/TONs- N_2 catalysts at deposition time of 30 min. Clearly we observe the formation of uniform spherical NiPt nanoparticles (average particle diameter equals 40 ± 5 nm) on the top of substrate and other smaller nanoparticles are deposited inside the TONs itself. However in case of TONs- N_2 the NiPt the nanoparticle packing (distribution) density is much higher than that in case of TONs-air substrate which can be related to the improvement in surface active sites and higher surface area of TONs- N_2 substrate [38]. The corresponding EDX analysis for NiPt/TONs-air and NiPt/TONs- N_2 SEM images are shown in Figure 3a and 3b respectively. The EDX analysis shows the presence of diffraction peaks for elemental Pt and Ni in addition to the peaks for TONs substrate. As shown in table 2 the atomic ratio of Ni: Pt equals 1.1:1 in case of TONs-air and 1: 1 in case of TONs- N_2 substrate which is consistent with the ratio of the plating bath composition of 1: 1.

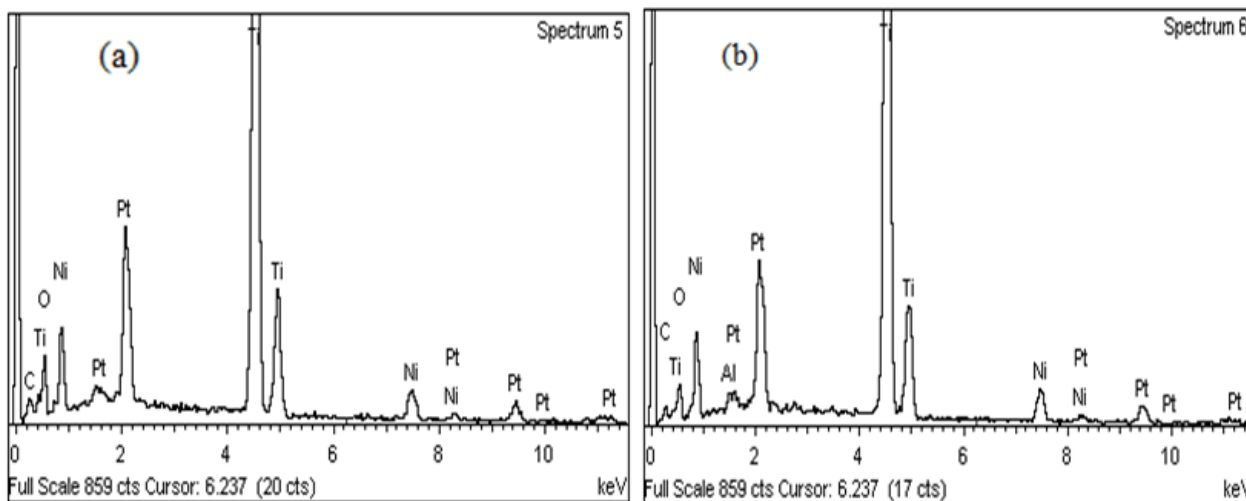


Figure 3. EDX spectrum (a) for NiPt/TONs-air and (b) EDX spectrum for NiPt/TONs-air

Table 2. EDAX analysis for Pt and Ni composition of NiPt/TONs catalysts

Catalyst	Element	Weight%	Atomic%
NiPtB/TONs-air	Ni	5.03	3.08
	Pt	14.76	2.72
NiPtB/TONs-N ₂	Ni	2.32	2.02
	Pt	7.59	1.99

The ICP-OES analysis was performed to define the amount of doped boron in NiPt catalysts by dissolving the alloy in HNO₃ using high-pressure microwave digestion system. The boron content in the catalyst was found to be about 0.098 ± 0.01 μg cm⁻². Figure 4 shows the X-ray diffraction patterns of the TONs-N₂ supported NiPt nanoparticles. There is no significant difference was observed for the XRD of TONs-air and TONs-N₂ indicating that they both have a similar crystal structure. The XRD in Figure 3 shows a distinctive diffraction peaks for fcc Pt and fcc Ni crystal structures. The diffraction peaks at 2θ = 44.5 and 76.4° can be assign to fcc nickel (111) and (222) diffraction planes while the peaks at 2θ = 40.9, 47.5 and 83.0 are designated to fcc Pt (111), (200) and (311) diffraction planes respectively.

The diffraction peaks of Pt in the XRD seem to be broadened and there are no noticeable peaks for phase separated structures such as a pure Ni or its oxides in the diffraction pattern. This indicates a good degree of alloying between Pt and Ni especially in case of NiPtB/TONs-N₂. In particular, the diffraction peaks were slightly shifted to the higher 2θ values in in case of NiPt catalyst as compared to those of the pure Pt particles which is in good agreement the literatures[41,42].

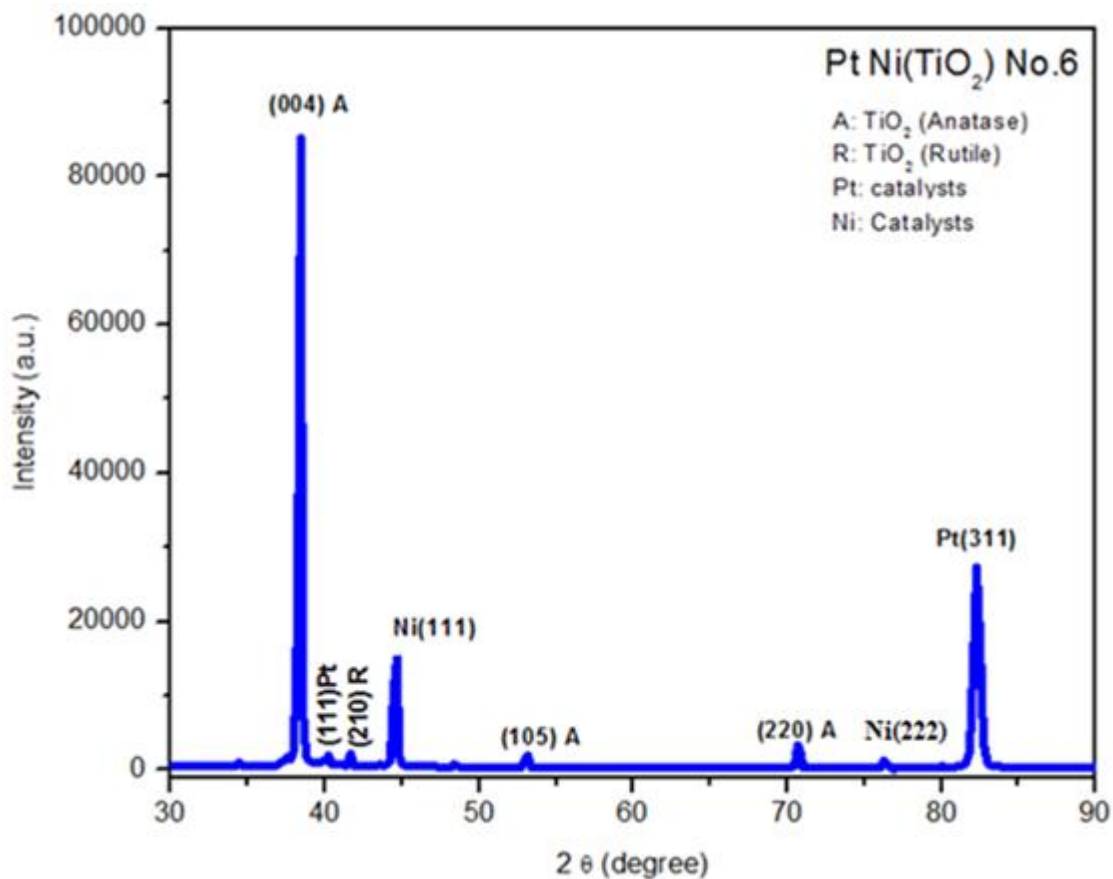


Figure 4. XRD patterns of NiPt/TONS-N₂ catalyst.

3.2 Electrochemical characterizations

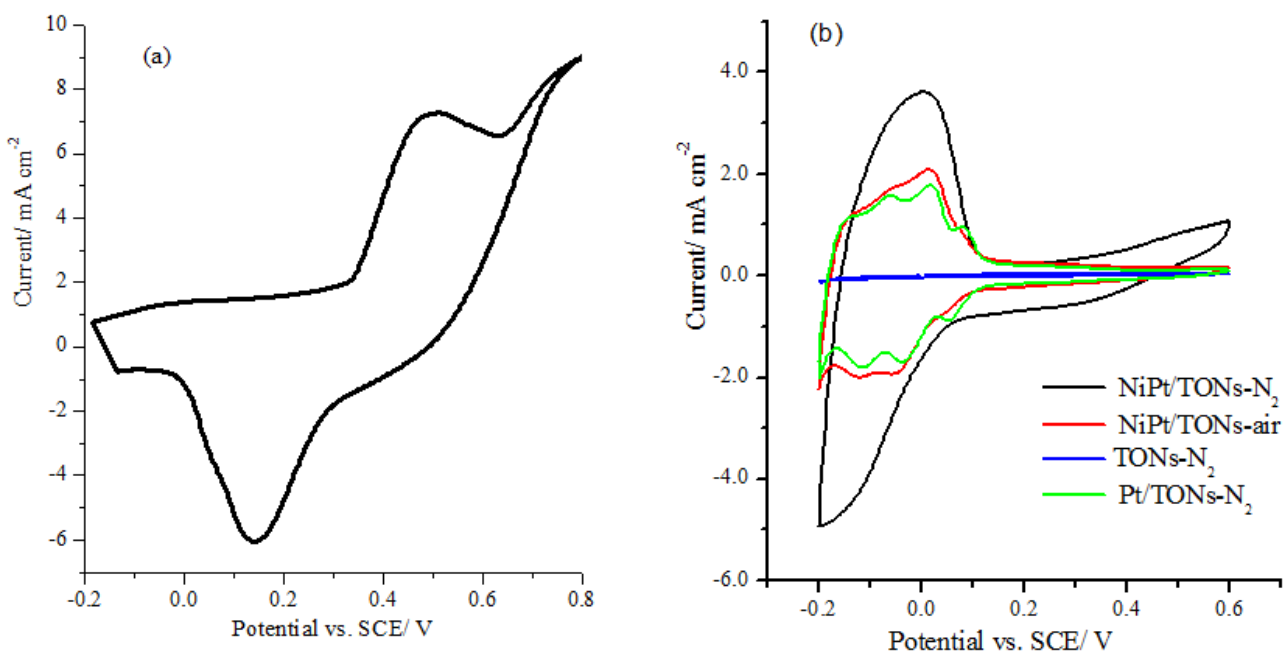


Figure 5. CVs at 50 mVs⁻¹ for (a) NiPt/TONS-N₂ in 1.0 M KOH and (b) TONS -N₂, NiPt/TONS-air, and NiPt-TONS-N₂ catalysts in 0.5 M H₂SO₄.

The electrochemical behavior of the annealed NiPt catalyst on the both substrates of TONs-air and TONs-N₂ were investigated by cyclic voltammetry (CV) in H₂SO₄ and KOH solutions. Figure 5 shows the CVs at 50 mV s⁻¹ for the NiPt/TONs-air and NiPt-TONs-N₂ catalysts measured in N₂ saturated solution of 0.5 M H₂SO₄ and 1.0 M KOH. For comparison the CVs for pure Pt/TONs-N₂ catalyst from our previous work is included [38]. The Pt/TONs-N₂ catalyst was chemically deposited by similar procedure but in absence of nickel precursor.

The cyclic voltammetry of NiPt/TONs-N₂ catalyst in alkaline solution in Figure 5a clearly shows well-resolved characteristic oxidation and reduction peaks at potentials of 0.40 V and 0.25 V vs. SCE, respectively, which related to the well-known redox couple of Ni²⁺/Ni³⁺ [43] reaction. In acidic solution (Figure 5b), the NiPt/TONs-N₂ catalyst showed much higher catalytic activity towards hydrogen adsorption-desorption than NiPt-TONs-air and Pt/TONs-N₂ catalysts. This can be attributed to a number of factors as reported by Loukrakpam et al. [44], which includes the lattice shrinking or lattice strain due to the changes in the Pt-Pt bond distance, D-band center shift and the Pt skin effect [45]. Additionally, the characteristics of the NiPt/TONs-air and NiPt/TONs-N₂ nanocatalysts can be understood based on the modification of the electronic properties of Pt by Ni and the synergistic role of Pt and Ni in the catalysts[46].

Table 3 shows the electrochemical surface area (ECSA) and roughness factor (R_f) for NiPt/TONs-air, NiPt-TONs-N₂ and Pt-B-TONs-N₂ catalysts as estimated from the charge under the hydrogen adsorption desorption peaks (Q_H). Evidently the NiPt/TONs-N₂ catalyst shows two times higher roughness than that for NiPt/TONs-air and Pt /TONs-N₂ which can attributed to the treatment of TONs support in nitrogen atmosphere significantly improved the conductivity and accessible surface area of NiPt catalyst.

Table 3. Electrochemical active surface area (ECSA) and roughness factors (R_F)

Catalyst	Q _H , mC	Surface area(cm ²)	R _f
NiPtB-TONs-N ₂	7.25	34.62	55.22
NiPtB-TONs-air	3.6	17.9	28.9
Pt-B-TONs-N ₂	3.73	17.76	26.11

3.3. Electrooxidation of methanol

The electro-catalytic performance of the NiPt/TONs-air and NiPt/TONs-N₂ catalysts was examined for methanol oxidation in alkaline and acidic solution by cyclic voltammetry. Figure 6 shows the CVs of NiPt/TONs-air and NiPt/TONs-N₂ catalyst electrodes at 50 mV s⁻¹ in 1.0 M KOH and in the presence of 0.5 M methanol. Again the CVs for pure Pt-TONs-N₂ catalyst (blue line) from our previous work is included for comparison. Obviously during the forward scan both catalysts show the characteristic methanol electrochemical oxidation peak around 0.0 V vs. SCE with NiPt/TONs-N₂ catalyst showing much higher oxidation current in comparison with Pt/TONs-N₂ and Pt/TONs-N₂

catalysts. The methanol oxidation peak potential is slightly shifted to more positive potential in case of NiPt/TONS-N₂ catalyst and the current densities reached 19.35, 10.4 and 15 mA cm⁻² for at NiPt/TONS-N₂, NiPt/TONS-air and Pt/TONS-N₂ respectively.

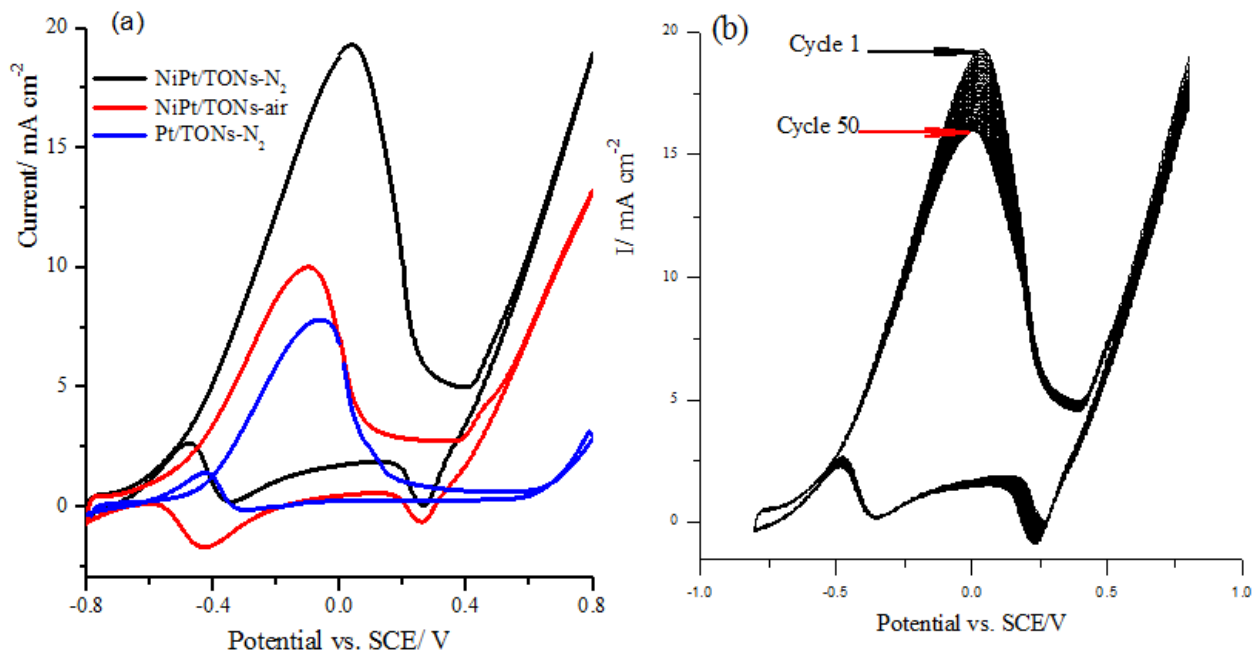


Figure 6. CVs at 50 mV s⁻¹ in 1.0 M KOH + 0.5 M CH₃OH for (a) NiPtB/TONS-N₂, NiPtB/TONS-air, and Pt/TiO₂NTs-N₂, (b) stability of the NiPtB/TONS-N₂ for 50 cycles.

The superior catalytic performance of NiPt/TONS-N₂ catalyst can be related to larger surface area, good dispersion of catalyst NPs, and higher electrical conductivity of TONS-N₂ substrate. The enhanced catalytic activity of NiPt/TONS catalysts in comparison with pure Pt-TONS may be attributed to the presence of Ni atoms, which changes the electronic structure of Pt and surface redox species of Ni oxide formed during the electro-oxidation process, which promotes the oxygenation of CO_{ads} [47].

Figure 6b shows the long-term cyclic stability of the NiPt/TONS-N₂ catalyst for methanol oxidation. The cyclic voltammetry shows a steady decrease in current density (about 8%) within the first 10 cycles, and then a nearly constant current density was gradually established for up to 50 cycles. This indicates that the NiPt/TONS-N₂ catalyst reveals higher catalytic activity and stability than NiPt/TONS-air and Pt/TONS-N₂ in alkaline media. The catalytic activity of the catalysts was also investigated in 0.5 M H₂SO₄ containing 0.5 M CH₃OH as shown in Figure 7. Both NiPt/TONS-N₂ and NiPt/TONS-air catalysts show a significant enhancement for methanol oxidation as compared to the Pt/TONS-N₂ and Pt/TONS-air catalysts, respectively.

Again, the long-term stability of NiPt-TONS-N₂ for oxidation of methanol in acidic solution is shown in Figure 7b. The catalyst shows a slightly decrease in peak current density (< 5%) during the first 10 cycles, then almost constant oxidation current density was reached at a longer time period.

The tolerance of a catalyst to intermediates generated during the oxidation of methanol used to be expressed by the ratio of peak currents of the anodic peaks in forward (I_f) and cathodic peak in the backward (I_b) scan[48].

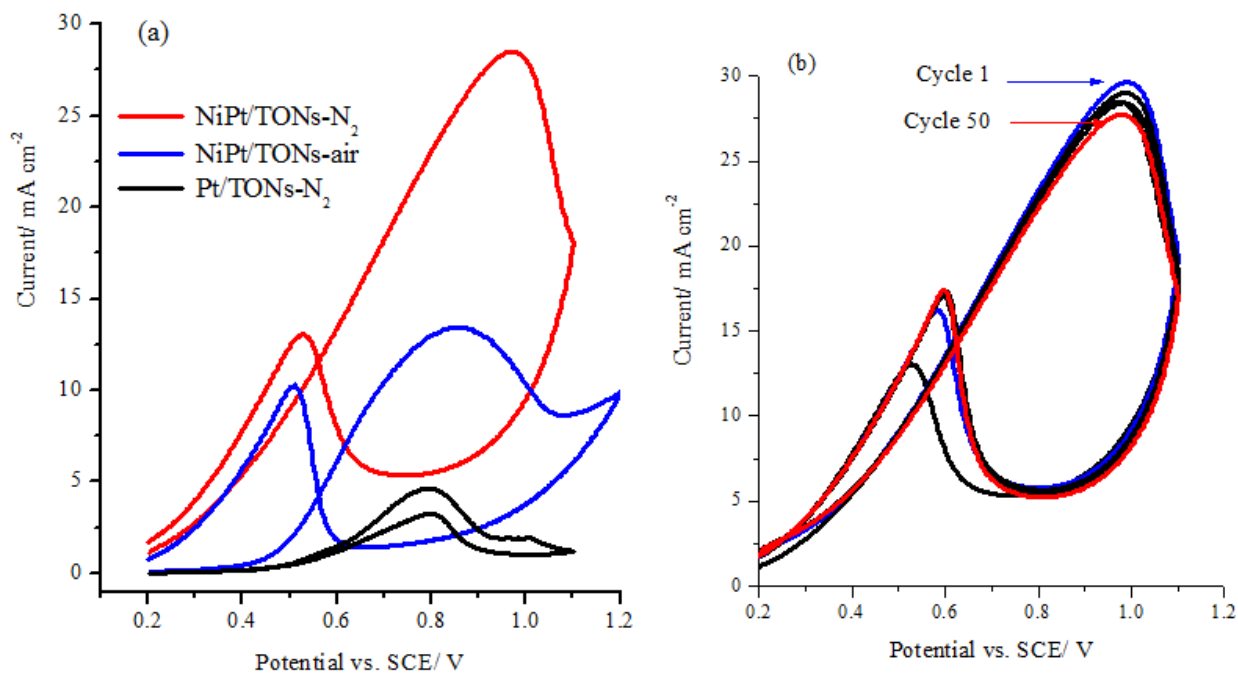


Figure 7. CVs of (a) the NiPtB/TONS-N₂, NiPtB/TONS-air, Pt-B/TONS-N₂ and Pt-B/TONS-air, (b) stability of the NiPtB/TONS-N₂ from first cycle to 50 cycles in 0.5 M H₂SO₄ + 0.5 M CH₃OH with a scan rate of 50 mVs⁻¹.

Table 4. A comparison of poison tolerance (I_f/I_b) of our catalysts with the ones in the literatures.

Catalysts	I_f/ mAcm^{-2}	I_b/ mAcm^{-2}	I_f/I_b	Reference
NiPt/TiO ₂ NTs-N ₂	28.3	12.70	2.22	This work
NiPt/TiO ₂ NTs-air	13.41	10.24	1.31	This work
Pt/TiO ₂ NTs-N ₂	4.58	3.24	1.41	40
Pt/C	0.75	1.0	0.75	50
NiPt/C	13.58	9.10	1.49	51
NiPt/C	0.66	0.59	1.12	52

A low I_f/I_b ratio indicates poor electrooxidation of methanol to carbon dioxide during the forward scan, and excessive accumulation of carbonaceous intermediates on the catalyst surface[49]. As shown in table 4, for NiPtB/TONs-N₂ catalyst, the value of I_f/I_b reaches 2.23, which is larger than that of the NiPtB/TONs-air (1.31) and Pt/TONs-N₂ (1.42) catalysts. Moreover, in comparison with the literature, our NiPtB/TONs-N₂ and Pt /TONs-N₂ catalysts shows much higher tolerance ratio (I_f/I_b) than that for NiPt and Pt catalysts supported on carbon. This finding again confirms that the high I_f/I_b ratio of NiPtB/TONs-N₂ related to the better conductivity of TONs-N₂ support and the higher surface area of the catalyst. In addition, the use of TONs-N₂ support reduces the absorption of carbonaceous intermediates at the catalyst surface during methanol oxidation.

5. CONCLUSION

In summary, the NiPt catalysts were chemically deposited at the surface and inside titanium oxides nanotubes (TONs) support which pre-fabricated by anodic oxidation of Ti foil in HF solution followed by annealing in air and in N₂ atmosphere. The produced NiPt/TONs catalysts have very uniform spherical nanoparticles with diameter less than 40 nm and Ni:Pt composition ratio of 1:1. In comparison similar catalysts supported on carbon, the NiPt/TONs catalysts show superior catalytic performance, and poison tolerance and stability towards methanol oxidation in acidic and alkaline solutions as studied by cyclic voltammetry. This was ascribed for the enhancement of surface area and TONs electrical conductivity due to the formation of favorable structure and surface defects. This work demonstrates that TONs is promising for use as a support for electrocatalysis applications.

ACKNOWLEDGEMENTS

This Project was supported by King Saud University, Deanship of Scientific Research, College of Science Research Center.

References

1. B. O'Regan, M. Gratzel, *Nature*, 353 (1991) 737-740.
2. A. Hagfeldt, M. Gratzel, *Acc. Chem. Research*, 33 (2000) 269.
3. F. Amano, T. Yasumoto, O. Prieto-Mahaney, S. Uchida, T. Shibayama, B. Ohtani, *Chem. Commun.*, 17 (2009) 2311-2313.
4. J. Zhu, J. Yang, Z. F. Bian, J. Ren, Y. M. Liu, Y. Cao, H. X. Li, H. Yong, K. N. Fan, *App. Catal. B: Environmental*, 76 (2007) 82-91.
5. A. Fujishima, K. Honda, *Nature*, 37 (1972), 238.
6. S. Bauer, A. Pittrof, H. Tsuchiya, P. Schmuki, *Electrochem. Commun.*, 13 (2011) 538.
7. M. Tian, M. Malig, S. Chen, A. Chen, *Electrochem. Commun.*, 13 (2011) 370.
8. C. Kormann, D. W. Bahnemann, M. R. Hoffmann, *Environ. Sci. Technol.*, 22 (1988) 798.
9. D. D. Dionysiou et al., *App. Cata. B: Environ.*, 125 (2012) 331.
10. D. Bavykin, E. Milsom, F. Marken, D. Kim, D. Marsh, D. Riley, F. Walsh, K. El-Abiary., A. Lapkin., *Electrochem Commun.*, 7 (2005) 1050-1058.
11. S. Liu, A. Chen, *Langmuir* 21 (2005) 8409.

12. E. Topoglidis, C. Campbell, A. Cass, J. Durrant, *Langmuir*, 17 (2001) 7899- 7906.
13. M. Grätzel, *Nature* 414 (2001) 338-344.
14. R. Vitiello, J. Macak, A. Ghicov, H. Tsuchiya, L. Dick, P. Schmuki, *Electrochem. Commun.* 8 (2006) 544.
15. A. Ghicov, J. Macak, H. Tsuchiya, J. Kunze, V. Haeublein, L. Frey, P. Schmuki, *Nano Lett.* 6 (2006) 1080-1082.
16. I. Paramasivam, J.M. Macak, P. Schmuki., 10 (2008) 71–75.
17. F. Wang, Z. Zheng, F. Jia, *Materials Letters* 71 (2012) 141–144.
18. Q. Liang, Z.D. Cui, S.L. Zhu, Y. Liu, X.J. Yang, *Journal of Catalysis* 278 (2011) 276–287.
19. S. Sakthivel, M. Shankar, M. Palanichamy, B. Arabindoo, D. Bahnemann, V. Murugesan. *Water Res.*, 38 (2004) 3001-3008.
20. I. Paramasivam, J.M. Macak, P. Schmuki, *Electrochemistry Communications*, 10 (2008) 71–75.
21. N. Deraz, M. Selim, M. Ramadan. *Mater Chem Phys.*, 113 (2009) 269–75.
22. H. He, P. Xiao, M. Zhou, Y. Zhang, Q. Lou, X. Dong, *Inter. J. Hydrogen*, 37 (201 2) 4967 -4973.
23. X. Li, J. Yaob, F. Liub, H. Heb, M. Zhoub, N. Mao, P. Xiao, Y. Zhang, *Sensors and Actuators B*, 181 (2013) 501– 508.
24. N. Tacconi, C. Boyles, K. Rajeshwar. *Langmuir*, 16 (2000) 5665–72.
25. S. Zhu, L.Wang, X. Zu, X. Xiang. *Appl Phys Lett.*, 88 (2006) 0431071–3.
26. P. Li, J. Liu, N. Nag, P. Crozier. *J Phys Chem B*, 109 (2005) 13883–90.
27. P. Li, J. Liu, N. Nag, P. Crozier. *Surf Sci.*, 600 (2006) 693–702.
28. Y. Takahashi, T. Tatsuma, *Langmuir*, 21 (2005) 12357.
29. Lian HQ, Wang JM, Xu L, Zhang LY, Shao HB, Zhang JQ, et al., *Electrochim Acta*, 56 (2011) 2074-2080.
30. O. Carp, C. Huisman, A. Reller. *Prog. Solid State Chem.*, 32 (2004) 33-177.
31. Z. Zhang, Y. Yuan, Y. Fang, L. Liang. *J Electroanal Chem.*, 610 (2007) 179.
32. B. Zhongqiu, X. Haixian, R. Jun, C. Lei, W. Yun, L. Haifeng, Z. Xingfu., *Materials Letters*, 124(2014)158–160.
33. J.M. Macak, F. Schmidt-Stein, P. Schmuki, *Elec. Communications*, 9 (2007) 1783-1787.
34. Z. Shengsen , W. Hongjuan, Y. Mingsang, F. Yueping, Y. Hao, P. Feng.. *Int. j. of hydrogen energy*, 38 (2013) 7241-7245.
35. W Sha, *Materials science; Metallurgy: Queen's University Electroless Copper and Nickel Phosphorus Plating*, ISBN: 978-1-84569-808-9 UK (2011).
36. A. Chiba, H. Haijima, W.C. Wu, *Ultrasonics* 42 (2004) 617-620.
37. S. A .Wasmus, J. Kuver., *Electroanal. Chem.*, 461 (1999) 14.
38. M.N. Shaddad, A. M. Al-Mayouf, M. A. Ghanem, M. S. AlHoshan, J. P. Singh, A. A Al-Suhybani *Int. J. Electrochem. Sci.*, 8 (2013) 2468 -2478.
39. M. A. Ghanem, J. P. Singh, A. M. Al-Mayouf, M N. Shaddad, M. Al-Hoshan, A. Al-Suhybani , *Electrocatalysis*, 4 (2013) 134-143.
40. G.Z. Cao, *Nanostructures & Nanomaterials*, Imperial College Press, London, 2004, p. 224.
41. S. Knupp, W. Li, O. Paschos, T. Murray, J. Snyder, P. Haldar, *Carbon*, 46 (2008) 1276.
42. T. Herricks, J. Chen, Y. Xia, *Nano Let.*, 4 (2004) 2367.
43. Y. Miao, L. Ouyang, S. Zhou, L. Xu, Z. Yang, M. Xiao, R. Ouyang, *Biosensors and Bioelectronics*, 53 (2014) 428–439.
44. R. Loukrakpam, J. Luo, T. He, Y. Chen, Z. Xu, P.N. Njoki, B.N. Wanjala, B. Fang, D. Mott, J. Yin, J. Klar, B. Powell, C.J. Zhong, *J. Phys. Chem. C*, 115 (2011) 1682–1694.
45. K.W. Park, J.H. Choi, Y.E. Sung, *J. of Physical Chemistry. B*, 107 (2003) 5851–5856.
46. P. Xiao, B.B. Garcia, Q. Guo, D.W. Liu, G.Z. Cao, *Elec. Communications*, 9 (2007) 2441–2447.
47. V.R. Stamenkovic, B. Fowler, B.S. Mun, G.F. Wang, P.N. Ross, C.A. Lucas, N.M. Markovic, *Science*, 315 (2007) 493–497.

48. V.R. Stamenkovic, B.S. Mun, M. Arenz, K.J.J. Mayrhofer, C.A. Lucas, G.F. Wang, P.N. Ross, N.M. Markovic, *Nat. Mater.*, 6 (2007) 241–247.
49. T.P. Moffat, J.J. Mallett, S.M. Hwang, *J. Electrochem. Soc.*, 156 (2009) B238–B251.
50. Y.N. Wu, S.J. Liao, Z.X. Liang, L.J. Yang, R.F. Wang, *J. Power Sources*, 194 (2009) 805.
51. Wang Yan, Zuo Shaoqing, Zhu Huaigong, *Trans. Tianjin Univ.*, 19 (2013) 436-439.
52. A. Nassr, S. Ilya, M.P. Marga, G. N. Wolfgang, B. Michael, *ACS Catal.*, 4 (2014) 2449–2462.

© 2015 The Authors. Published by ESG (www.electrochemsci.org). This article is an open access article distributed under the terms and conditions of the Creative Commons Attribution license (<http://creativecommons.org/licenses/by/4.0/>).